Intravenously Injected [1-^{14}C]Arachidonic Acid Targets Phospholipids, and [1-^{14}C]Palmitic Acid Targets Neutral Lipids in Hearts of Awake Rats

Eric J. Murphy[1],*, Thad A. Rosenberger, Casey B. Patrick, and Stanley I. Rapoport

Section on Brain Physiology and Metabolism, National Institute on Aging, National Institutes of Health, Bethesda, Maryland 20892-1582

ABSTRACT: The differential uptake and targeting of intravenously infused [1-^{14}C]palmitic ([1-^{14}C]16:0) and [1-^{14}C]arachidonic ([1-^{14}C]20:4n-6) acids into heart lipid pools were determined in awake adult male rats. The fatty acid tracers were infused (170 μCi/kg) through the femoral vein at a constant rate of 0.4 mL/min over 5 min. At 10 min postinfusion, the rats were killed using pentobarbital. The hearts were rapidly removed, washed free of exogenous blood, and frozen in dry ice. Arterial blood was withdrawn over the course of the experiment to determine plasma radiotracer levels. Lipids were extracted from heart tissue using a two-phase system, and total radioactivity was measured in the nonvolatile aqueous and organic fractions. Both fatty acid tracers had similar plasma curves, but were differentially distributed into heart lipid compartments. The extent of [1-^{14}C]20:4n-6 esterification into heart phospholipids, primarily choline glycerophospholipids, was elevated 3.5-fold compared to [1-^{14}C]16:0. The unilateral incorporation coefficient, *k**, which represents tissue radioactivity divided by the integrated plasma radioactivity for heart phospholipid, was sevenfold greater for [1-^{14}C]20:4n-6 than for [1-^{14}C]16:0. In contrast, [1-^{14}C]16:0 was esterified mainly into heart neutral lipids, primarily triacylglycerols (TG), and was also found in the nonvolatile aqueous compartment. Thus, in rat heart, [1-^{14}C]20:4n-6 was primarily targeted for esterification into phospholipids, while [1-^{14}C]16:0 was targeted for esterification into TG or metabolized into nonvolatile aqueous components.

Paper no. L8403 in *Lipids 35,* 891–898 (August 2000).

While it is well-established that phospholipid breakdown is accelerated during myocardial ischemia (1–3), until recently the roles of phospholipids and their constitutive fatty acids in lipid-mediated signal transduction and membrane turnover in the heart were poorly understood. A number of signal transduction mechanisms in the heart function through a phospholipase A_2-mediated release of arachidonic acid (20:4n-6). In rat ventricular myocytes, interleukin-1β (IL-1β) activates the plasmalogen selective phospholipase A_2 through a receptor-linked mechanism, resulting in increased 20:4n-6 levels (4). Tumor necrosis factor-α also increases phospholipase A_2 activity in rat ventricular myocytes, although the phospholipase A_2 which is activated is apparently different from that activated by IL-1β (5). Angiotensin II stimulates the release of both 20:4n-6 and inositol phosphates through activation of multiple receptor subtypes involving increased phospholipase A_2 and phospholipase C activity (6). The β_2-adrenergic receptor stimulation leads to 20:4n-6 release through activation of a cytosolic phospholipase A_2 (7). Furthermore, the heart has an active phosphoinositide pathway that responds to α-1-adrenergic and muscarinic receptor stimulation (8,9). This pathway is partially regulated by lysophosphatidylcholine levels, with its activity decreasing with increasing levels (10). This suggests that, lysophosphatidylcholine produced by phospholipase A_2-mediated hydrolysis of choline glycerophospholipids (ChoGpl) regulates another lipid-mediated signal transduction system in the heart. Despite the role of 20:4n-6 in heart lipid-mediated signal transduction, the uptake and targeting of this fatty acid in the heart are controversial.

The mammalian heart uses palmitic acid (16:0) as a primary source of metabolic energy *via* β-oxidation (11), but the heart also takes up polyunsaturated fatty acids such as 20:4n-6 (12). The uptake rate and ultimate deposition of fatty acids depend, in part, upon chain length (11). Palmitic acid, a saturated fatty acid, is targeted for esterification into triacylglycerol (TG) pools and used to meet energy demands (11, 13). Oleic acid, a monounsaturated fatty acid, is also taken up by heart and is targeted for esterification into TG (14). Uptake and targeting of these fatty acids toward β-oxidation are decreased with high glucose levels (15). However, when glucose levels are in the physiologic range, saturated and monounsaturated fatty acids are esterified into TG and used almost exclusively for β-oxidation (13–15).

In contrast, the ultimate fate of 20:4n-6 in heart is unclear. A number of studies in isolated hearts or isolated myocytes

[1]National Research Council Senior Fellow.

*To whom correspondence should be addressed at Section on Brain Physiology and Metabolism, National Institute on Aging, National Institutes of Health, Building 10, Room 6C103, Bethesda, MD 20892.
E-mail: murphye@mail.nih.gov

Abbreviations: CE, cholesteryl esters; CerPCho, sphingomyelin; ChoGpl, choline glycerophospholipids; DG, diacylglycerols; EtnGpl, ethanolamine glycerophospholipids; FFA, free fatty acids; IL-1β, interleukin-1β; *k**, unilateral incorporation coefficient; PET, positron emission tomography; PlsCho, choline; PlsEtn, ethanolamine plasmalogen; PtdIns, phosphatidylinositol; PtdOH, phosphatidic acid; PtdSer, phosphatidylserine; TG, triacylglycerols; TLC, thin-layer chromatography.

suggest that esterification of 20:4n-6 into lipid pools is concentration-dependent (12,16). For instance, in a perfused isolated heart model, when the concentration of 20:4n-6 in the perfusate is high, it is preferentially esterified into myocyte TG (12,16), while when the concentration is low, it is preferentially esterified into phospholipids (12). Regardless, very little 20:4n-6 is used for β-oxidation, thereby conserving this fatty acid for other uses (12). This conservation is consistent with the utilization of 20:4n-6 in lipid-mediated signal transduction. Other studies in myocytes have shown that 20:4n-6 and other polyunsaturated fatty acids are esterified into the TG pool much more than into phospholipid pools (17). Under these experimental conditions, the heart did not elongate or desaturate the fatty acids, suggesting that it lacks the high levels of enzymic activity for these functions (17). Results also indicate that 20:4n-6 found in heart is not formed from linoleic acid but rather arises from direct uptake from the circulation (17). Thus, the targeting of 20:4n-6 in heart remains unclear. These conflicting results suggest that 20:4n-6 uptake and targeting need to be reexamined in the heart.

Others have used perfused heart models or isolated myocytes to study 20:4n-6 uptake and targeting, but these models may not represent the situation found *in vivo*. Therefore, we examined 20:4n-6 uptake and targeting, as compared to 16:0, by intravenously infusing awake adult male rats with either [1-^{14}C]20:4n-6 or [1-^{14}C]16:0 and quantifying the uptake and deposition of each tracer into different heart lipid pools. By using high specific activity tracers, unlabeled plasma fatty acid levels were unaltered (18). We found that [1-^{14}C]20:4n-6 was largely esterified into rat heart phospholipids, whereas [1-^{14}C]16:0 was preferentially esterified into heart TG and found in the nonvolatile aqueous fraction representing by-products of β-oxidation.

MATERIALS AND METHODS

Animals. Male Sprague-Dawley rats (200 g) were obtained from Charles River Laboratories (Wilmington, DE) and maintained *ad libitum* on standard laboratory rat chow and water prior to surgery. This study was conducted in accordance with the National Institutes of Health Guidelines for the Care and Use of Laboratory Animals (NIH publication 80-23), under a protocol approved by the National Institute of Child Health and Development's Institutional Animal Care and Use Committee.

Animal surgery. Unfasted rats were anesthetized with respired halothane (1–3%), and their femoral artery and vein were catherized with polyethylene tubing (PE-50). Following catheter insertion, the wound was closed using standard surgical staples and the area anesthetized with xylocaine (1%). The rats were wrapped in plaster body casts, taped to wooden blocks, and maintained postoperatively in a quiet temperature-controlled environment that kept body temperature at 37°C for 3 h prior to infusion. Seven out of eight rats survived (88%) the surgical procedure.

Awake rats were infused with 170 μCi/kg of either [1-^{14}C]20:4n-6 or [1-^{14}C]16:0 into the femoral vein over 5 min, using a constant rate infusion pump (Harvard Apparatus Co., South Natick, MA). Throughout the experimental period, arterial blood samples (200 μL) were taken to determine plasma radioactivity. Fifteen minutes from the start of infusion, the rats were killed using sodium pentobarbital (100 mg/kg, i.v.). The hearts were rapidly removed, bisected, and residual blood was removed by rinsing with ice-cold 0.9% KCl. After blotting, the hearts were frozen in dry ice.

Preparation of radiotracer. Radiotracers (Moravek Biochemical, Brea, CA) were prepared by taking an aliquot of either tracer in ethanol and evaporating the ethanol under a constant stream of N_2 at 50°C. Radiotracer purity was assessed by thin-layer chromatography (TLC) and found to be >97% pure for each tracer. The fatty acid tracers were individually solubilized in 5 mM HEPES (pH 7.4) buffer containing fatty acid free-bovine serum albumin (50 mg/mL; Sigma Chemical Co., St. Louis, MO). Solubilization was facilitated by sonication in a bath sonicator for 10 min. Radioactivity was determined using liquid scintillation counting and adjusted to 100 μCi/mL. The appropriate amount of radiotracer was prepared for each animal to administer 170 μCi/kg (18).

Plasma extraction. Arterial blood samples, taken at predetermined time points during the infusion period, were stored on ice for up to 10 min before separating the plasma by centrifugation using a Beckman microfuge (Fullerton, CA). Plasma lipids were extracted by transferring a 100-μL aliquot of plasma into a tube containing 3 mL of chloroform/methanol (2:1, vol/vol), then vortexing. The addition of 0.63 mL of 0.9% KCl to these tubes resulted in two phases, which were thoroughly mixed and allowed to separate overnight in a −20°C freezer. The upper phase was removed and the lipid-containing lower phase was rinsed with 0.63 mL of theoretical upper phase to remove any water-soluble contaminants (19). Phase separation was facilitated by centrifugation at 1500 rpm and 0°C in a refrigerated Sorvall RT 6000 B centrifuge (DuPont Instruments, Wilmington, DE). The upper phase was discarded, the lower phase was dried, and its radioactivity quantified using a Packard 2200 CA Tricarb liquid scintillation counter (Packard Instruments, Downers Grove, IL).

Heart extraction. Frozen heart tissue was weighed, minced, and extracted in a Tenbroeck tissue homogenizer using a two-phase system (19). Briefly, the tissue mass (g) was multiplied by a correction factor of 1.28 to convert it to an equivalent value expressed in mL (20). This value represented 1 vol. The minced tissue was placed in the homogenizer and 17 vol of chloroform/methanol (2:1, vol/vol) added. Tissue was homogenized to a fine particulate-like powder. The solvent was removed and the homogenizer rinsed with 2 vol of chloroform/methanol (2:1, vol/vol). The rinse was added to the original sample, and 4 vol of 0.9% KCl solution added to this combined lipid extract. After vigorous mixing, phase separation was facilitated by centrifugation as described above. The upper phase and proteinaceous interface were removed and saved in a 20-mL glass scintillation vial. The lower organic phase was washed twice with 2 mL of theoretical upper phase, with phase separation facilitated by cen-

trifugation between washes. The washes were removed and combined with the previously removed upper phase. The washed lower phase was dried under a stream of nitrogen and the lipids redissolved in 1 mL of *n*-hexane/2-propanol (3:2, vol/vol) containing 5.5% H_2O.

Aqueous fraction. The aqueous fraction was processed for liquid scintillation counting by first being dried at 80°C for 18 h to remove $^{14}CO_2$. The dried material was then solubilized in 2 mL of Soluable (Packard Instruments) in tightly capped scintillation vials heated at 80°C for 2 h. Radioactivity was determined after addition of 10 mL of Ready-Solv (Beckman Instruments) using a Packard 2200 CA Tricarb liquid scintillation counter.

TLC. Phospholipids and neutral lipids were separated by TLC. For each separation, 100 µL of sample was spotted onto a TLC plate. Phospholipids were separated on heat-activated Whatman silica gel-60 plates (20 × 20 cm, 250 µm) developed in chloroform/methanol/acetic acid/water (60:30:3:1, by vol). This solvent system resolves cardiolipin, phosphatidic acid (PtdOH), and ethanolamine glycerophospholipids (EtnGpl) but not phosphatidylinositol (PtdIns) and phosphatidylserine (PtdSer). Neutral lipids were separated using heat-activated silica G plates (Analtech, Newark, DE) developed in petroleum ether/diethyl ether/acetic acid (70:30:1.3, by vol) (21). This solvent system resolves cholesteryl esters (CE) and TG. Lipid fractions were determined using authentic standards (Doosan-Serday, Englewood Cliffs, NJ, and Nu-Chek-Prep, Elysian, MN).

Bands corresponding to PtdOH, EtnGpl, combined PtdIns/PtdSer, ChoGpl, and sphingomyelin (CerPCho) were scraped into 20-mL liquid scintillation vials, and 0.5 mL H_2O was added followed by 10 mL of Beckman Ready-Solv. After mixing, the samples were quantified by liquid scintillation counting at least 1 h after the addition of the Ready-Solv. Bands corresponding to TG, CE, diacylglycerol (DG), and free fatty acids (FFA) also were scraped into 20-mL scintillation vials and counted as described above.

Plasmalogens. Fatty acid esterification into choline and ethanolamine plasmalogen was also determined. ChoGpl and EtnGpl were separated by TLC, the phospholipids removed by scraping, and the phospholipids extracted from the silica using *n*-hexane/2-propanol (3:2, vol/vol) containing 5.5% H_2O. The extraction was 97–98% efficient based on the recovery of radioactivity. The ChoGpl and EtnGpl fractions were dried under a stream of nitrogen and exposed to HCl vapor for 15 min to hydrolyze the vinyl ether linkage (22). The samples were redissolved in solvent, and the acid-labile and -stable fractions were separated by high-performance liquid chromatography (22) and collected in 20-mL scintillation vials. The solvent was evaporated and the radioactivity determined as described above.

Unilateral incorporation coefficient of labeled fatty acid. Integrated areas for the plasma radioactivity curves were determined using the trapezoidal method (Sigma Plot; Jandel Scientific, San Rafael, CA). Total radioactivity for each individual heart fraction was normalized to the wet weight (g ww) and divided by the integrated area of plasma radioactivity. This calculation essentially normalizes the tissue radioactivity to the exposure of plasma tracer. The resulting coefficient is called the unilateral incorporation coefficient or k^*, with values expressed as s^{-1} (23). Hence, the k^* represents the radioactivity of each fraction normalized to the amount of presented radioactivity in the plasma. The following equation was used to calculate the k^*:

$$k^* = c^*_{\text{tissue}} \Big/ \int_0^T c^*_{\text{plasma}}\, dt \qquad [1]$$

where k^* = incorporation coefficient of tracer into a heart compartment, c^*_{tissue} = tracer radioactivity in the heart compartment, c^*_{plasma} = tracer radioactivity in the plasma, and T = time of tissue sampling.

Statistical analysis. Statistical analysis was done using a two-tailed Student's *t*-test or one-way analysis of variance coupled with Tukey-Kramer multiple comparisons test when appropriate. Statistical significance was defined at $P < 0.05$. For the [^{14}C]20:4n-6 group, $n = 4$, and for the [^{14}C]16:0 group, $n = 3$. Data are given as means ± standard deviation.

RESULTS

Plasma curves. Infusion of [1-^{14}C]20:4n-6 or [1-^{14}C]16:0 for 5 min produced a rapid increase in total organic plasma radioactivity, followed by a decline in radioactivity which was indistinguishable between the two tracers (Fig. 1). Tracer plasma half-lives were 81 ± 1 and 79 ± 1 s for [1-^{14}C]20:4n-6 and [1-^{14}C]16:0, respectively. The average areas under the curve were also equivalent, 1061 ± 223 and 1184 ± 59 nCi × mL plasma^{-1} × min^{-1} for [1-^{14}C]20:4n-6 and [1-^{14}C]16:0, respectively. The bulk of this radioactivity (>95%) was found in the plasma FFA fraction, with only minor amounts found esterified to plasma lipids (data not shown).

[1-^{14}C]16:0 and [1-^{14}C]20:4n-6 radioactivity. Total radioactivity of [1-^{14}C]20:4n-6 and [1-^{14}C]16:0 in heart tissue, 15 min after infusion began, was determined by measuring the radioactivity in the combined organic and dried aqueous phases (Table 1). Total radioactivity for [1-^{14}C]20:4n-6 was twofold greater than for [1-^{14}C]16:0. In the lipid-containing organic fraction, [1-^{14}C]20:4n-6 radioactivity was threefold higher relative to [1-^{14}C]16:0. There was no significant difference between radioactivities in the dried aqueous phase.

TABLE 1
Incorporated [1-^{14}C]16:0 and [1-^{14}C]20:4n-6 into Rat Heart[a]

	Radioactivity (µCi/g ww)		
	Total	Aqueous (nonvolatile)	Organic
[^{14}C]16:0 ($n = 3$)	0.34 ± 0.11	0.14 ± 0.06	0.20 ± 0.13
[^{14}C]20:4n-6 ($n = 4$)	0.68 ± 0.18*	0.06 ± 0.02	0.61 ± 0.19*

[a]Values represent means ± SD. *Statistical significance, $P < 0.05$, using a two-tailed Student's *t*-test. Abbreviation: ww, wet weight.

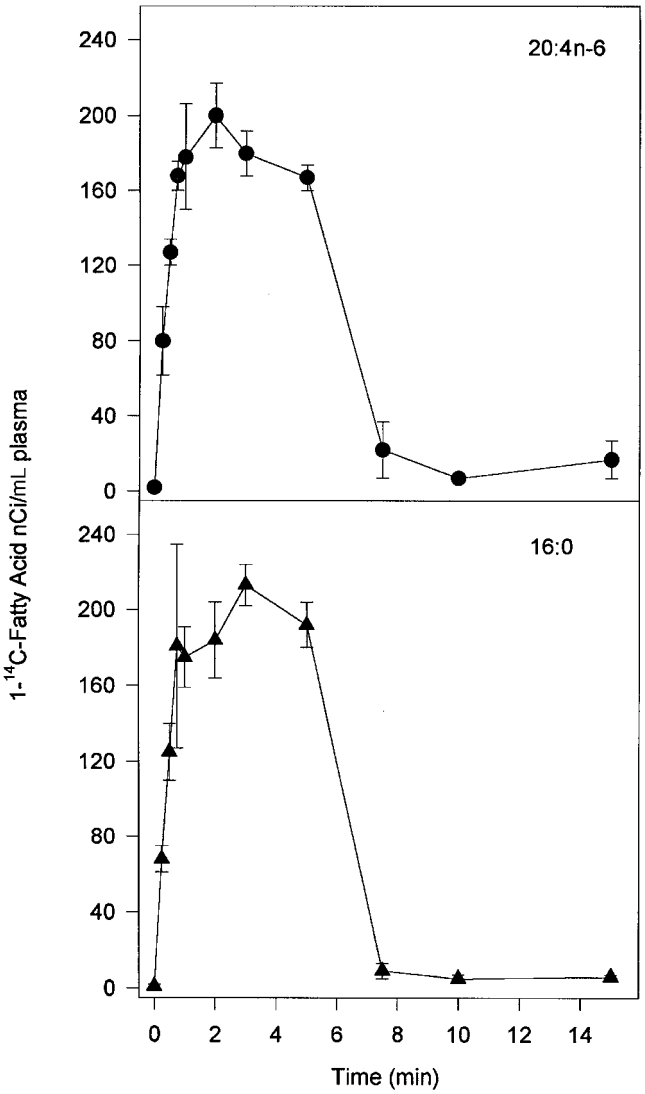

FIG. 1. Plasma curves for [1-^{14}C]20:4n-6 and [1-^{14}C]16:0. Values are expressed as nCi/mL plasma and represent means ± SD, $n = 3$.

Thus, [1-^{14}C]20:4n-6 was found primarily in the organic fraction, where 91% of the total tissue radioactivity was found. For [1-^{14}C]16:0, 60% of the total tissue radioactivity was found in the organic fraction. Furthermore, calculating the percentage extraction of each radiotracer by the heart from the total amount infused, the percentage oxidation was 0.37 ± 0.11 and 0.16 ± 0.06% ($P = 0.0292$) for 20:4n-6 and 16:0, respectively.

k*. The differences between [1-^{14}C]20:4n-6 and [1-^{14}C]-16:0 levels in heart may have arisen from preferential fatty acid extraction from plasma. To assess this possibility, radioactivity in different heart compartments was normalized to net exposure to plasma tracer, by calculating the unilateral incorporation coefficient for each tracer, *k** (Eq. 1). The *k** was calculated for total heart (combined organic and nonvolatile aqueous fractions), the lipid-containing organic fraction, and for the nonvolatile aqueous compartments (Table 2). The organic fraction was then fractionated into phospholipid, esterified neutral lipid, and FFA fractions, and *k** were calculated for these pools (Table 2). In the total heart, *k** was 2.2-fold greater for [1-^{14}C]20:4n-6 than for [1-^{14}C]16:0. There was no significant difference between the tracers in *k** in the aqueous compartment. For the organic fraction, *k** was 3.3-fold greater for [1-^{14}C]20:4n-6 than for [1-^{14}C]16:0. When the organic fraction was divided into its phospholipid and esterified neutral lipid compartments, differences were very apparent (Table 2). In the phospholipid fraction, *k** was 7.5-fold greater for [1-^{14}C]20:4n-6 than for [1-^{14}C]16:0. In the FFA compartment, *k** was over fivefold greater for [1-^{14}C]20:4n-6 than for [1-^{14}C]16:0. It was difficult to ascertain whether this increase in free [1-^{14}C]20:4n-6 represented fatty acid available for esterification or fatty acid that had been released by phospholipase A_2 during heart removal. There was no significant difference between the *k** for each tracer for the neutral lipid fraction. In any case, [1-^{14}C]20:4n-6 was more rapidly incorporated into the heart organic fraction than was [1-^{14}C]16:0, and this disparity was largely accounted for by a 7.5-fold greater *k** into heart phospholipids.

Incorporation coefficients were then calculated for different lipid classes (Table 3). In the phospholipids, *k** was larger for [1-^{14}C]20:4n-6 than for [1-^{14}C]16:0 in all fractions except PtdOH. Most notable was a 12.3-fold greater *k** for incorporation into the ChoGpl. Similar in magnitude was the ninefold greater *k** for [1-^{14}C]20:4n-6 relative to [1-^{14}C]16:0 in the combined PtdIns/PtdSer fraction. In esterified neutral lipids, the only difference was in the DG fraction, where *k** for [1-^{14}C]20:4n-6 was fivefold greater than that for [1-^{14}C]16:0. The values of *k** for the individual lipid classes confirm that [1-^{14}C]20:4n-6 was incorporated selectively into the phospholipid classes and that there was no difference between *k** for [1-^{14}C]20:4n-6 and [1-^{14}C]16:0 into neutral lipid fractions except for the DG fraction.

Distribution of [1-^{14}C]16:0 and [1-^{14}C]20:4n-6. The percentage distribution of radioactive fatty acids that were esterified into the neutral and phospholipid fractions was calculated by dividing an individual *k** by total *k** (Table 2). A significantly greater percentage of [1-^{14}C]20:4n-6 was esterified into the total phospholipid fraction compared to [1-^{14}C]16:0. In contrast, the percentage of [1-^{14}C]16:0 esterified into neutral lipids was threefold greater than that for [1-^{14}C]20:4n-6, despite a similar incorporation coefficient (Table 2). A greater percentage of [1-^{14}C]20:4n-6 was found as unesterified or free fatty acid compared to [1-^{14}C]16:0. These results confirm the selective targeting of [1-^{14}C]20:4n-6 for esterification into phospholipids, while [1-^{14}C]16:0 was targeted for esterification into neutral lipids.

To better understand these differences, the phospholipid and neutral lipid fractions were further separated into individual classes, and the percentage distribution of individual values of *k** relative to total *k** was determined (Table 3). For the neutral lipids, [1-^{14}C]16:0 was found primarily in TG. The percentage of [1-^{14}C]16:0 in the TG was increased 7.2-fold greater than for [1-^{14}C]20:4n-6. Distribution of radioactivity into CE was not significantly different between the radiola-

TABLE 2
Unilateral Incorporation Coefficient, *k, and Distribution of Total Radioactivity for Fractions from Rat Heart[a]**

	$k^* \times 10^{-3}$		Total k^* (%)	
	[^{14}C]16:0	[^{14}C]20:4n-6	[^{14}C]16:0	[^{14}C]20:4n-6
Fractions[b]				
Total	4.91 ± 1.78	10.68 ± 1.77*		
Organic	2.91 ± 2.02	9.59 ± 1.78*	56.0 ± 21.1	89.8 ± 6.7*
Aqueous	2.03 ± 0.82	1.09 ± 0.71	44.0 ± 21.1	10.2 ± 6.7*
Organic fraction[c]				
Phospholipid	0.87 ± 0.46	6.51 ± 0.91*	17.6 ± 5.0	61.4 ± 5.8*
Neutral lipid	1.67 ± 1.45	0.87 ± 0.17	31.0 ± 16.2	8.1 ± 0.7*
Free fatty acid	0.36 ± 0.13	1.89 ± 0.51*	7.5 ± 2.1	17.5 ± 3.4*

[a]Incorporation coefficients are expressed as s^{-1} and represent means ± SD. Percentage of total k^* was calculated by dividing individual k^* for each fraction by the total k^* and represents means ± SD. *Statistical significance, $P < 0.05$, using a two-tailed Student's *t*-test.
[b]Values under this heading represent distribution of radioactivity in all of the fractions.
[c]Values under this heading represent the major fraction found in the organic fraction under the heading "Fractions."

beled fatty acids, although there was a 2.5-fold increase in the percentage of [1-^{14}C]20:4n-6 in the DG fraction compared to [1-^{14}C]16:0. Whether this DG fraction represents an anabolic or catabolic intermediate is not clear.

Because [1-^{14}C]20:4n-6 was found mainly in phospholipids (Table 3), the distribution of radioactive fatty acids into individual phospholipid classes was evaluated. In the ChoGpl, the percentage of [1-^{14}C]20:4n-6 was 5.7-fold greater than for [1-^{14}C]16:0. Similarly, in the combined PtdIns/PtdSer fraction, [1-^{14}C]20:4n-6 percentages were increased 4.3-fold over the percentage of [1-^{14}C]16:0 in the same fraction. The smallest difference was seen in the CerPCho fraction, while the EtnGpl fractions were not different between groups. Thus, [1-^{14}C]20:4n-6 was preferentially targeted for esterification into phospholipids and found primarily in the ChoGpl fraction.

The vast proportion of heart arachidonic acid is found in choline and ethanolamine plasmalogens (24,25). To determine if [1-^{14}C]20:4n-6 and [1-^{14}C]16:0 were also targeted to the plasmalogens, the distributions of [1-^{14}C]20:4n-6 and of [1-^{14}C]16:0 in choline (PlsCho) and ethanolamine plasmalogens (PlsEtn) were measured. Only a small proportion of either fatty acid tracer was found in plasmalogen subclasses. For PlsEtn, 1.6 ± 0.1% and 1.9 ± 0.7% of total heart radioactivity was found in this subclass for [1-^{14}C]20:4n-6 and [1-^{14}C]16:0, respectively. In the PlsCho subclass, 2.4 ± 0.6 and 2.2 ± 1.7% of the total radioactivity were present for the [1-^{14}C]20:4n-6 and [1-^{14}C]-16:0 infused rats, respectively. These results indicate that within the 15-min time frame of this study, there was limited pulse labeling of plasmalogens by either fatty acid tracer.

TABLE 3
Unilateral Incorporation Coefficients, *k, and Distribution of Radioactivity for Individual Lipid Classes[a]**

	$k^* \times 10^{-3}$		Total k^* (%)	
	[^{14}C]16:0	[^{14}C]20:4n-6	[^{14}C]16:0	[^{14}C]20:4n-6
Phospholipids				
EtnGpl	0.32 ± 0.16	0.74 ± 0.19*	6.5 ± 1.9	6.9 ± 0.8
ChoGpl	0.41 ± 0.19	5.04 ± 0.70*	8.4 ± 2.4	47.6 ± 5.1*
PtdIns/PtdSer	0.06 ± 0.04	0.54 ± 0.09*	1.2 ± 0.3	5.1 ± 0.8*
PtdOH	0.04 ± 0.02	0.05 ± 0.03	0.5 ± 0.3	0.5 ± 0.3
CerPCho	0.03 ± 0.01	0.13 ± 0.03*	0.5 ± 0.1	1.3 ± 0.3*
Neutral lipids				
TG	1.52 ± 1.33	0.42 ± 0.10	28.0 ± 14.9	3.9 ± 0.3*
DG	0.08 ± 0.04	0.40 ± 0.09*	1.6 ± 0.6	3.8 ± 0.5*
CE	0.08 ± 0.08	0.04 ± 0.03	1.5 ± 1.1	0.4 ± 0.2

[a]Incorporation coefficients are expressed as s^{-1} and represent means ± SD. Percentage of total k^* was determined by dividing individual compartment k^* by the total k^* and represents means ± SD. *Statistical significance, $P < 0.05$, using a two-tailed Student's *t*-test. Abbreviations: EtnGpl, ethanolamine glycerophospholipids; ChoGpl, choline glycerophospholipids; PtdIns, phosphatidylinositol; PtdSer, phosphatidylserine; PtdOH, phosphatidic acid; CerPCho, sphingomyelin; TG, triacylglycerols; DG, diacylglycerols; CE, cholesteryl esters.

DISCUSSION

Because of the increasing recognition of the importance of phospholipids and their fatty acids in heart function and structure (4,5,8,10, 26,27), we quantified incorporation coefficients and targeting of [1-^{14}C]20:4n-6 and [1-^{14}C]16:0 in heart, using intravenous infusion of tracer in awake adult male rats. Previously, this method was used to quantify fatty acid incorporation and turnover rates for various fatty acids in the brains of awake adult rats (28,29). Because the quantity of radiotracer injected does not alter the plasma concentration of the infused fatty acid, this model avoids artifacts that may result from elevating plasma fatty acid levels above normal physiological levels (18,23,29). This avoids possible problems related to the observed concentration dependence for 20:4n-6 targeting in isolated hearts and myocytes (12,16,17).

In heart, saturated and monounsaturated fatty acids are utilized as the primary energy source, consistent with the fact that the heart has a tremendous capacity for fatty acid uptake and esterification (11,15). Palmitic acid is targeted for esterification into TG pools (12,13,16) or is used for β-oxidation directly (16). Oleic acid is also targeted to neutral lipids; nearly 80% of the oleic acid is localized in TG in both isolated perfused hearts and isolated myocytes (14). Our results confirm that 16:0 is preferentially esterified into the neutral lipid compartment, with the neutral lipids accounting for over 30% of the total radioactivity and into the nonvolatile aqueous pool accounting for 44% of the total radioactivity (Table 2). However, in contrast to other reports, we found nearly 18% of total [1-^{14}C]16:0 esterified into the heart phospholipid pools (Table 2). This value is similar to that reported in isolated myocytes, where 18% of the fatty acid is found in myocyte phospholipids, although this distribution in myocytes was not calculated from total radioactivity; thus the contribution of the aqueous radioactivity to the total radioactivity was not included (12). In isolated working rat heart, 9.5% of 16:0 in the lipid fraction is esterified into heart phospholipids (16). This value is not very different from ours, considering the difference in models. Thus, although [1-^{14}C]16:0 was esterified into heart phospholipids in awake rats, it was primarily targeted to the neutral lipid fraction where it was esterified into TG, or it was metabolized to products found in the nonvolatile aqueous phase.

In various isolated heart models and myocyte preparations, 20:4n-6 uptake and targeting appear to be linked to fatty acid availability (12,16,17). In isolated working rat heart, nearly all 20:4n-6 taken up from the perfusate (20:4n-6 concentration 1.2 mM) enters TG, with only 14% going into phospholipids (16). However, the 20:4n-6 concentration used in this study (16) is supraphysiologic, as the free 20:4n-6 concentration in rats *in vivo* is on the order of 16 μM (30). Consistent with these observations, much lower concentrations of 20:4n-6 (0.02–0.4 μM) are targeted almost exclusively in isolated rat myocytes to TG (82.3%), whereas only 12.3% is esterified into phospholipids (17). However, in isolated adult rat myocytes, 39% of the labeled 20:4n-6 in the lipid fraction is found in phospholipids when the medium 20:4n-6 concentration is 20 μM, but at a medium concentration of 5 nM; over 71% of the labeled 20:4n-6 is esterified into phospholipids (12). Clearly, targeting of 20:4n-6 is concentration-dependent in these models, suggesting a need to reevaluate 20:4n-6 uptake and targeting in an intact awake animal using physiologically relevant concentrations of each fatty acid.

In contrast to published results, we report that [1-^{14}C]-20:4n-6 was targeted selectively into heart phospholipids (60% of total radioactivity) in awake adult male rats (Table 2) and found primarily in ChoGpl (Table 3). Only 9% of the total radiotracer in heart at 15 min was found in the nonvolatile aqueous phase, compared with nearly 41% for [1-^{14}C]16:0. This suggests that [1-^{14}C]20:4n-6 was minimally metabolized to water-soluble nonvolatile compounds and was conserved relative to [1-^{14}C]16:0. Using the same fatty acid model, nearly 40% of the [1-^{14}C]16:0 found in the brain following infusion had been metabolized to slowly-disappearing nonvolatile aqueous phase compounds, mainly glutamate and aspartate (31). In rats infused with [20-^{18}F]20:4n-6 at radiotracer levels, 72.9% of the labeled 20:4n-6 in heart was found in the organic fraction and the majority of that radioactivity in the phospholipid fraction (32). In isolated heart models or myocytes, 20:4n-6 also appears to be conserved (12) and minimally metabolized by β-oxidation (12,17). Our data support these results. We also found that [1-^{14}C]20:4n-6 had a greater incorporation coefficient and was taken up to a greater extent by the heart than [1-^{14}C]16:0 (Tables 1 and 2), although our calculations did not take into account the complete conversion of 16:0 to CO_2. The published values for plasma fatty acid concentrations are 16.1 ± 0.9 and 161.3 ± 7.0 nmol × mL^{-1} for 20:4n-6 and 16:0, respectively (30), a 10-fold difference in the cold fatty acid concentrations. Using the unilateral incorporation coefficient determined in this study (Table 2), the incorporation of cold 20:4n-6 and 16:0 was 0.152 ± 0.002 and 0.758 ± 0.011 nmol × mL^{-1} × s^{-1} ($P <$ 0.0001), respectively. This is only a fivefold difference in uptake despite a 10-fold difference in availability, suggesting that there are selective processes for the uptake of 20:4n-6 from the plasma. These results indicate that in awake rats, relatively more cold 20:4n-6 appeared to have been extracted by the heart from the plasma than cold 16:0 and that this extracted 20:4n-6 was mainly esterified into phospholipids, despite a 10-fold greater availability of cold 16:0 in the plasma (30).

One mechanism that may explain the differential targeting of [1-^{14}C]20:4n-6 and [1-^{14}C]16:0 in heart could be the different affinities of CoA-dependent and -independent acyltransferase and transacylases for these two fatty acids (33). In rabbit heart, a cytosolic CoA-dependent acyltransferase exists which selectivity acylates 20:4n-6 onto ChoGpl (34). This might explain our observation that [^{14}C]20:4n-6 was preferentially esterified into ChoGpl (Table 3). Furthermore, this enzyme is highly selective for 20:4n-6 and is not found in the liver, suggesting it is localized solely in heart (34). In contrast, the CoA-independent acyltransferase does not exhibit

any substrate selectivity (34), suggesting that our observed differences in fatty acid targeting were accounted for by a heart-specific, 20:4n-6 selective, cytosolic CoA-dependent acyltransferase, which targets fatty acids primarily into ChoGpl.

The importance of the ethanolamine and choline plasmalogen subclasses in lipid-mediated signal transduction has become more apparent in heart since the isolation and characterization of a plasmalogen-selective phospholipase A_2 from heart (35–37). Further, because the plasmalogen subclass comprises a large proportion of ChoGpl and EtnGpl in mammalian heart (24,25,38,39) and because the *sn*-2 position contains a large proportion of heart 20:4n-6, we determined [1-^{14}C]20:4n-6 distribution into the PlsCho and PlsEtn. In awake rats, very little (<3%) [1-^{14}C]20:4n-6 was esterified into the PlsCho or PlsEtn. A plausible explanation for these results is that ether lipid biosynthesis *de novo* proceeds at a rate in heart that is much slower than the experimental time frame used. Indeed, heart plasmalogen biosynthesis *de novo* occurs on the order of hours, with no newly formed plasmalogen evident until up to 3 h after infusion of [1-^{3}H]-hexadecanol (40). This certainly may account for the minimal amount of [1-^{14}C]20:4n-6 found in the plasmalogens if the majority of the 20:4n-6 is esterified into plasmalogens during the synthetic process as opposed to esterification into lysoplasmenylcholine or to a direct transfer by a transacylase (33).

Lastly, because of the preferential targeting of [1-^{14}C]-20:4n-6 to phospholipid pools and the lack of appreciable alternative metabolism *via* other pathways, [^{11}C]20:4n-6 infusion coupled with positron emission tomography (PET) could be used to clinically study dynamic phospholipid turnover in heart. Past human heart studies using [^{11}C]palmitate with PET scanning have focused on the β-oxidation aspect of myocardial fatty acid metabolism (41,42); however, our findings suggest that these studies could be extended to examine lipid-mediated signal transduction in diseased human heart using [^{11}C]20:4n-6.

In summary, upon entering the heart, [1-^{14}C]20:4n-6 was predominantly esterified into ChoGpl, while [1-^{14}C]16:0 was targeted for esterification into TG or found in the nonvolatile aqueous fraction. The k^* for phospholipids was sevenfold greater for [1-^{14}C]20:4n-6 compared to [1-^{14}C]16:0, while there was no difference in values of k^* for esterified neutral lipids. Thus, in the awake adult rat, where the normal plasma fatty acid levels were maintained, there was a differential targeting of [1-^{14}C]20:4n-6 and [1-^{14}C]16:0 into distinct heart lipid pools. This suggests that fatty acid targeting in heart is based upon function. Further, this differential targeting suggests that 20:4n-6 and 16:0 have substantially different roles in heart metabolism and function.

ACKNOWLEDGMENTS

We thank Cindy Murphy for the typed preparation of this manuscript. This work was supported in part by a senior fellowship awarded by the National Research Council to EJM.

REFERENCES

1. Gunn, M.D., Sen, A., Chang, A., Willerson, J.T., Buja, L.M., and Chien, K.R. (1985) Mechanisms of Accumulation of Arachidonic Acid in Cultured Myocardial Cells During ATP Depletion, *Am. J. Physiol. 249*, H1188–H1194.
2. Freyss-Beguin, M., Millanvoye-Van Brussel, E., and Duval, D. (1989) Effect of Oxygen Deprivation on Metabolism of Arachidonic Acid by Cultures of Rat Heart Cells, *Am. J. Physiol. 257 (Heart Circ. 26)*, H444–H451.
3. Miyazaki, Y., Gross, R.W., Sobel, B.E., and Saffitz, J.E. (1990) Selective Turnover of Sarcolemmal Phospholipids with Lethal Cardiac Myocyte Injury, *Am. J. Physiol. 259 (Cell Physiol. 28)*, C325–C331.
4. McHowat, J., and Liu, S. (1997) Interleukin-1β Stimulates Phospholipase A_2 Activity in Adult Rat Ventricular Myocytes, *Am. J. Physiol. 272 (Cell Phys. 41)*, C450–C456.
5. Liu, S.J., and McHowat, J. (1998) Stimulation of Different Phospholipase A_2 Isoforms by TNF-α and IL-1β in Adult Rat Ventricular Myocytes, *Am. J. Physiol. 275 (Heart Circ. 44)*, H1462–H1472.
6. Lokuta, A.J., Cooper, C., Gaa, S.T., Wang, H.E., and Rogers, T.B. (1994) Angiotensin II Stimulates the Release of Phospholipid-Derived Second Messengers Through Multiple Receptor Subtypes in Heart Cells, *J. Biol. Chem. 269*, 4832–4838.
7. Pavoine, C., Magne, S., Sauvadet, A., and Pecker, F. (1999) Evidence for a β2-Adrenergic/Arachidonic Acid Pathway in Ventricular Cardiomyocytes. Regulation by the β1-Adrenergic/cAMP Pathway, *J. Biol. Chem. 274*, 628–637.
8. Meij, J.T.A., and Lamers, J.M.J. (1989) Alpha-1-adrenergic Stimulation of Phosphoinositide Breakdown in Cultured Neonatal Rat Ventricular Myocytes, *Mol. Cell Biochem. 88*, 73–75.
9. de Chaffoy de Courcelles, D. (1989) Is There Evidence of a Role of the Phosphoinositol-Cycle in the Myocardium? *Mol. Cell Biochem. 88*, 65–72.
10. Liu, S.-Y., Yu, C.-H., Hays, J.-A., Panagia, V., and Dhalla, N.S. (1997) Modification of Heart Sarcolemmal Phosphoinositide Pathway by Lysophosphatidylcholine, *Biochim. Biophys. Acta 1349*, 264–274.
11. DeGrella, R.F., and Light, R.J. (1980) Uptake and Metabolism of Fatty Acids by Dispersed Adult Rat Heart Myocytes. I. Kinetics of Homologous Fatty Acids, *J. Biol. Chem. 255*, 9731–9738.
12. Hohl, C.M., and Rosen, P. (1987) The Role of Arachidonic Acid in Rat Heart Cell Metabolism, *Biochim. Biophys. Acta 921*, 356–363.
13. Klein, M.S., Goldstein, R.A., Welch, M.J., and Sobel, B.E. (1979) External Assessment of Myocardial Metabolism with [^{11}C]Palmitate in Rabbit Hearts, *Am. J. Physiol. 237*, H51–H57.
14. Tamboli, A., O'Looney, P., Vander Maten, M., and Vahouny, G.V. (1983) Comparative Metabolism of Free and Esterified Fatty Acids by the Perfused Rat Heart and Rat Cardiac Myocytes, *Biochim. Biophys. Acta 750*, 404–410.
15. DeGrella, R.F., and Light, R.J. (1980) Uptake and Metabolism of Fatty Acids by Dispersed Adult Rat Heart Myocytes. II. Inhibition of Albumin and Fatty Acid Homologues, and the Effect of Temperature and Metabolic Reagents, *J. Biol. Chem. 255*, 9739–9745.
16. Saddik, M., and Lopaschku, G.D. (1991) The Fate of Arachidonic Acid and Linoleic Acid in Isolated Working Rat Hearts Containing Normal or Elevated Levels of Coenzyme A, *Biochim. Biophys. Acta 1086*, 217–224.
17. Hagve, T.-A., and Sprecher, H. (1989) Metabolism of Long-Chain Polyunsaturated Fatty Acids in Isolated Cardiac Myocytes, *Biochim. Biophys. Acta 1001*, 338–344.
18. Freed, L.M., Wakabayashi, S., Bell, J.M., and Rapoport, S.I. (1994) Effect of Inhibition of β-Oxidation on Incorporation of

[U-^{14}C]Palmitate and [1-^{14}C]Arachidonate into Brain Lipids, *Brain Res. 645*, 41–48.
19. Folch, J., Lees, M., and Sloane-Stanley, G.H. (1957) A Simple Method for the Isolation and Purification of Total Lipids from Animal Tissues, *J. Biol. Chem. 226*, 497–509.
20. Radin, N.S. (1988) Lipid Extraction, in *Neuromethods 7 Lipids and Related Compounds* (Boulton, A.A., Baker, G.B., and Horrocks, L.A., eds.) pp. 1–62, Humana Press, Clifton, NJ.
21. Marcheselli, V.L., Scott, B.L., Reddy, T.S., and Bazan, N.G. (1988) Quantitative Analysis of Acyl Group Composition of Brain Phospholipids, Neutral Lipids, and Free Fatty Acids, in *Neuromethods 7 Lipids and Related Compounds* (Boulton, A.A., Baker, G.B., and Horrocks, L.A., eds.) pp. 83–110, Humana Press, Clifton, NJ.
22. Murphy, E.J., Stephens, R., Jurkowitz-Alexander, M., and Horrocks, L.A. (1993) Acidic Hydrolysis of Plasmalogens Followed by High-Performance Liquid Chromatography, *Lipids 28*, 565–568.
23. Kimes, A.S., Sweeney, D., London, E.D., and Rapoport, S.I. (1983) Palmitate Incorporation into Different Brain Regions in the Awake Rat, *Brain Res. 274*, 291–301.
24. Gross, R.W. (1984) High Plasmalogen and Arachidonic Acid Content of Canine Myocardial Sarcolemma: A Fast Atom Bombardment Mass Spectroscopic and Gas Chromatography–Mass Spectroscopic Characterization, *Biochemistry 23*, 158–165.
25. Gross, R.W. (1985) Identification of Plasmalogen as the Major Phospholipid Constituent of Cardiac Sarcoplasmic Reticulum, *Biochemistry 24*, 1662–1668.
26. Kang, J.X., Xiao, Y.-F., and Leaf, A. (1995) Free, Long-Chain, Polyunsaturated Fatty Acids Reduce Membrane Electrical Excitability in Neonatal Rat Cardiac Myocytes, *Proc. Natl. Acad. Sci. USA 92*, 3997–4001.
27. Honore, E., Barhanin, J., Attali, B., Lesage, F., and Lazdunski, M. (1994) External Blockade of the Major Cardiac Delayed-Rectifier K^+ Channel (Kv1.5) by Polyunsaturated Fatty Acids, *Proc. Natl. Acad. Sci. USA 91*, 1937–1944.
28. Rapoport, S.I., Purdon, D., Shetty, H.U., Grange, E., Smith, Q., Jones, C., and Chang, M.C.J. (1997) *In Vivo* Imaging of Fatty Acid Incorporation into Brain to Examine Signal Transduction and Neuroplasticity Involving Phospholipids, *Ann. NY Acad. Sci. 620*, 56–74.
29. Robinson, P.J., Noronha, J., DeGeorge, J.J., Freed, L.M., Nariai, T., and Rapoport, S.I. (1992) A Quantitative Method for Measuring Regional *in vivo* Fatty Acid Incorporation into and Turnover Within Brain Phospholipids: Review and Critical Analysis, *Brain Res. Rev. 17*, 187–214.
30. Chang, M.C.J., Bell, J.M., Purdon, A.D., Chikhale, E.G., and Grange, E. (1999) Dynamics of Docosahexaenoic Acid Metabolism in the Central Nervous System: Lack of Effect of Chronic Lithium Treatment, *Neurochem. Res. 24*, 399–406.
31. Gnaedinger, J.M., Miller, J.C., Latker, C.H., and Rapoport, S.I. (1988) Cerebral Metabolism of Plasma [^{14}C]Palmitate in Awake Adult Rat: Subcellular Localization, *Neurochem. Res. 13*, 21–29.
32. Nagatsugi, F., Hokazono, J., Sasaki, S., and Maeda, M. (1996) 20-[^{18}F]Fluoroarachidonic Acid: Tissue Biodistribution and Incorporation into Phospholipids, *Biol. Pharm. Bull. 19*, 1316–1321.
33. Yamashita, A., Sugiura, T., and Waku, K. (1997) Acyltransferases and Transacylases Involved in Fatty Acid Remodeling of Phospholipids and Metabolism of Bioactive Lipids in Mammalian Cells, *J. Biochem. 122*, 1–16.
34. Needleman, P., Wyche, A., Sprecher, H., Elliott, W.J., and Evers, A. (1985) A Unique Cardiac Cytosolic Acyltransferase with Preferential Selectivity for Fatty Acids That Form Cyclooxygenase/Lipooxygenase Metabolites and Reverse Essential Fatty Acid Deficiency, *Biochim. Biophys. Acta 836*, 267–273.
35. Hazen, S.L., Stuppy, R.J., and Gross, R.W. (1990) Purification and Characterization of Canine Myocardial Cytosolic Phospholipase A_2. A Calcium-Independent Phospholipase with Absolute *sn*-2 Regiospecificity for Diradyl Glycerophospholipids, *J. Biol. Chem. 265*, 10622–10630.
36. Hazen, S.L., and Gross, R.W. (1991) ATP-Dependent Regulation of Rabbit Myocardial Cytosolic Calcium-Independent Phospholipase A_2, *J. Biol. Chem. 266*, 14526–14534.
37. Hazen, S.L., and Gross, R.W. (1993) The Specific Association of a Phosphofructokinase Isoform with Myocardial Calcium-Independent Phospholiase A_2. Implications for the Coordinated Regulation of Phospholipolysis and Glycolysis, *J. Biol. Chem. 268*, 9892–9900.
38. Das, D.K., Maulik, N., and Jones, R.M. (1994) Gas Chromatography–Mass Spectroscopic Detection of Plasmalogen Phospholipids in Mammalian Heart, in *Lipid Chromatographic Analysis* (Shibamoto, T., ed.) pp. 317–345, Marcel Dekker, Inc., New York.
39. Scherrer, L.A., and Gross, R.W. (1989) Subcellular Distribution, Molecular Dynamics and Catabolism of Plasmalogens in Myocardium, *Mol. Cell Biochem. 88*, 97–105.
40. Ford, D.A., and Gross, R.W. (1994) The Discordant Rates of *sn*-1 Aliphatic Chain and Polar Head Group Incorporation into Plasmalogen Molecular Species Demonstrate the Fundamental Importance of Polar Head Remodeling in Plasmalogen Metabolism in Rabbit Myocardium, *Biochemistry 33*, 1216–1222.
41. Geltman, E.M. (1994) Assessment of Myocardial Fatty Acid Metabolism with 1-^{11}C-Palmitate, *J. Nucl. Cardiol. 1*, S15–S22.
42. Lerch, R.A., Ambos, H.D., Bergmann, S.R., Welch, M.J., Ter-Pogossian, M.M., and Sobel, B.E. (1981) Localization of Viable, Ischemic Myocardium by Positron-Emission Tomography with ^{11}C-Palmitate, *Circulation 64*, 689–699.

[Received November 30, 1999, and in final revised form May 4, 2000; revision accepted June 22, 2000]